

# UltraGraph Optics Design

5/10/99

Jim Hagerman

## Introduction

This paper presents the current design status of the UltraGraph optics. Compromises in performance were made to reach certain product goals. Cost, size, and simplicity are favored in the overall scheme because UltraGraph is targeting a broad market. It is far more profitable to sell a thousand units at low cost than a single unit at high cost.

The prime market for UltraGraph is for scientific use with microscopes. UG is designed to be useful for research in biology and medicine where simultaneous spatial and spectral information is desired. Many features were added to make the instrument as flexible as possible for other applications, including low noise and low light capability (astronomy & fluorescence), adaptable fore-optic mounting, high resolution, cooling, eyepiece, battery power, tripod mount, etc. The product brochure is attached at the end of this document.

## Architecture

After considering several possible spectrograph configurations, the simplest and lowest cost was an Ebert-Fastie type. Fig. 1 shows a side view of the basic instrument layout. Fore-topics are attached at the right using a Nikon F type (bayonet) mount. This mount was selected because of the excellent optics available and that most microscopes and telescopes already have existing adapter accessories. For space-borne or other applications that do not need an eyepiece or have unusual fore-optics, the entire front part of UG is removable.

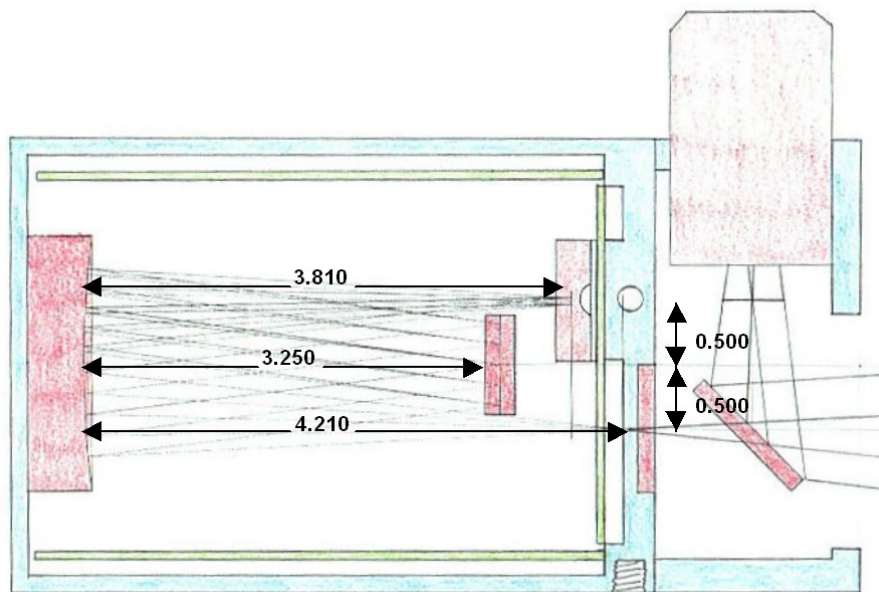
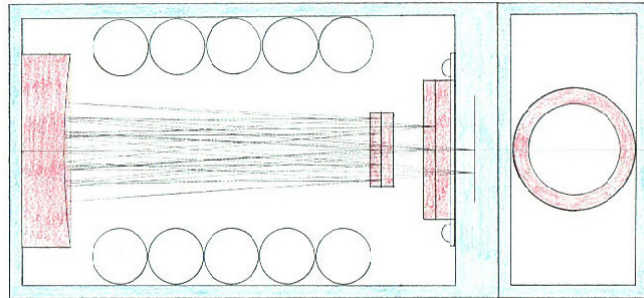


Figure 1. Ultragraph layout from side.

A flip mirror (motorized) also acts as a shutter. Next optic is a low pass filter to cutoff any UV light under 290nm. The slit is positioned under the CCD sensor board on the main structural surface/heat sink. The primary mirror is a 2" f/2 spherical which columnates the light onto the grating. The light is reflected back

(using order +1) onto the primary mirror again and finally focused onto the CCD. The nominal optic spacing is given. The circuit board on the bottom contains the camera controller electronics, and the board on top is the power supply. On both sides are battery backs, see Fig. 2. They will all need to be treated (painted black?) to reduce stray light.



**Figure 2. Top view of layout.**

The main reason why such a simple and low cost spectrograph design works is because of the very high working F-numbers. Most telescopes work at  $f/10$  and a microscope is about  $f/14$ , angles of 2.86 and 2.0 degrees respectively. Such small cone angles result in a large depth of field and reduced aberrations. Fig. 3 shows the light ray path for order +1. The dispersion is set to match the CCD which is 58 by 512 pixels. The spectrum was chosen to fit into 58 bands of 10nm each. With  $24\mu\text{m}$  square pixels that means the dispersion over 580nm is 1.368mm. This is extremely low dispersion and for this design requires a grating groove density of 23/mm.

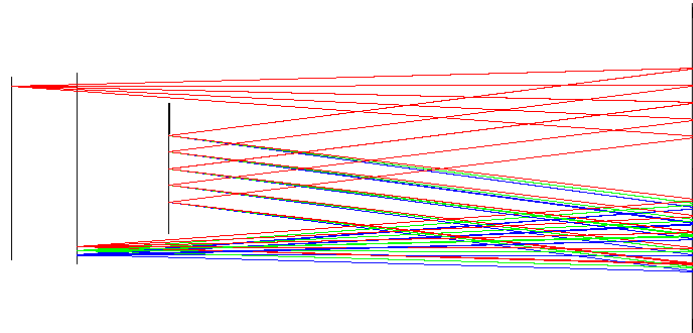


**Figure 3. Ray tracing of optical path.**

A high resolution mode was added by ruling the opposite side of the grating at 230/mm. The motorized grating angle then provides a 1nm per pixel resolution (addressability) mode.

To simplify mechanics, the object and image points are at different focal lengths. The slit was pushed behind the circuit board hanging on the CCD (which mounts directly to the heat sink surface). The slit mounts directly to the heat sink itself (reference surface). The grating is pushed as far back as possible while still having clearance to rotate through 360 degrees.

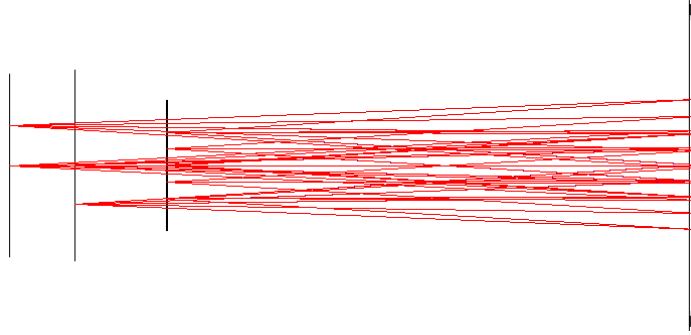


**Figure 4. Top view of optical path.**

### Dispersion

The CCD detector chosen (Hamamatsu S7031-0906) has an incredibly wide spectral response and UG was designed to make the most of it. Fore-optics and grating efficiency would effectively reduce the range but it seemed reasonable to push into the UV down to about 300nm and out to the NIR at 1 $\mu$ m. Of course, the visible region would have priority. With 58 channels it worked out nicely to center at 580nm (green) which gives a 290nm to 870nm response. A second range from 435nm to 1015nm is also possible with a different grating position. In hi-res mode the full 290nm to 1015nm is possible (more about that later).

The wavelength position at the focal plane is determined by grating angle. For small angles the translation is reasonably linear. Fig. 5 shows the optics in hi-res mode with 1nm per pixel dispersion. It is clear that some wavelengths will hit the grating and reflect back onto the primary causing stray light problems.

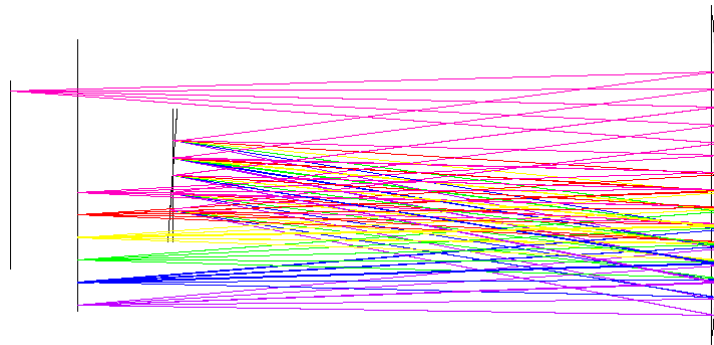


**Figure 5. Dispersion in hi-res mode.**

The wavelengths shown in Fig. 5 are 290nm, 435nm, 580nm, 725nm, 870nm, and 1015nm. Dispersion should be 13.68mm. Using Zemax, Fig. 6 shows the low-res mode dispersion using 23/mm density at the focal plane.

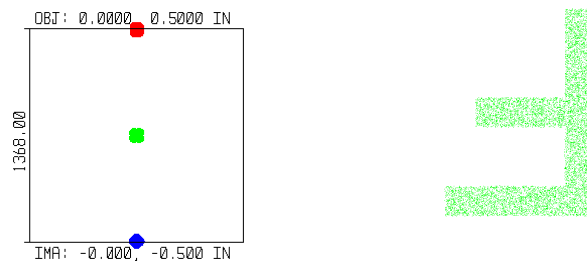


**Figure 6. Dispersion of wavelengths at CCD and orientation.**

Another compromise to be looked at is the use of an off-the-shelf master grating which has 25 grooves/mm. The spectral spacing would then be about 9nm per pixel. The grating mirror angles for various wavelengths to hit the center of the CCD in hi-res mode are given in the following table.

wavelength (nm)	tangent( $\gamma$ )
290	0.035
435	0.052
580	0.69
725	0.868
870	0.1045
1015	0.1225

From this and other simulations the average linear dispersion was calculated to be 0.123mrad/pixel. Since the grating will be controlled by a stepper motor, this equates to 51,100 steps per rotation. If a stepper motor with 18 degree steps is used, then a gear ratio of 2,555:1 is needed. Unfortunately, the required drive is not constant but should be something like an arcsine function which is not possible with a stepper motor. Such a compromise results in some spectral errors and smearing at the edges of the band (UV, and NIR) where the position error across the CCD is up to 3%.

Another problem is that of order mixing. Normally spectrometers are limited to a single octave of operation because the higher orders of diffraction mix with the lower ones. Fig. 7 shows how they overlap at every doubling of wavelength.

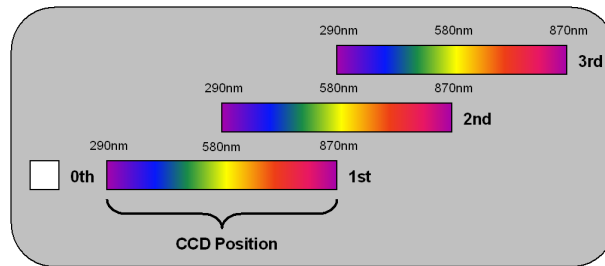


**Figure 7. Spectral order mixing.**

The 0<sup>th</sup> order doesn't mix with anything and is designed to miss the CCD in normal operation. UG uses an optimized +1 order. It is seen that the 2<sup>nd</sup> order overlaps the 1<sup>st</sup> starting at 580nm. The 290nm UV cutoff filter sets this limit. Therefore, a 400nm signal will also show up in the 800nm bin but at a lesser efficiency. The spectrum in the 1<sup>st</sup> order from 290nm to 580nm is unmixed and pure. It is hoped that by knowing or calibrating the relative operating efficiencies of UG that this 2<sup>nd</sup> order mixing can be subtracted out in post processing. It is not perfect but may perform well enough for many applications. If not, then the application must add an external low pass filter (which we, of course, will sell) of a more appropriate wavelength. Each application can optimize for a given octave when very high SNRs are required.

## TDI

The hi-res mode is accomplished using an innovative technique. The spectrum scanning (grating rotation) is made synchronous to the parallel clocking of the CCD. This is a TDI (time delay integration) mode of operation relative to the spectrum. Although only 58 bands are sensed at any one time, eventually, the entire 290nm to 1015nm bandwidth is scanned. Fig. 8 shows TDI operation.

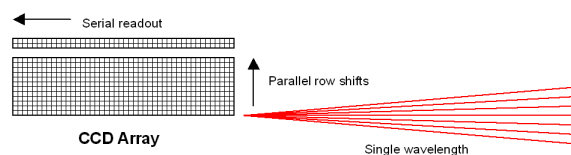


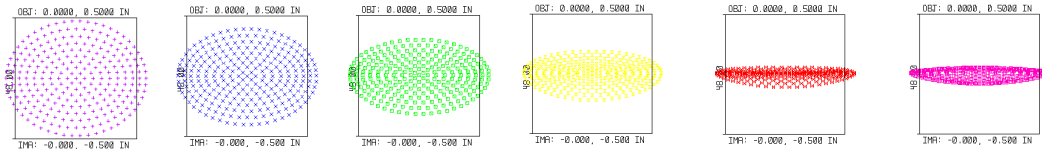
**Figure 8. TDI spectral operation.**

As mentioned earlier, the 3% positional error across the CCD at the ends of the band result in a 2 pixel smear in TDI. Therefore, the spectral resolution is cut to essentially 2nm bins at the extremes.

Another trick UG will employ is that of modulated TDI/scanning. The clocking speed will be varied inversely in proportion to the known efficiency. That is, clocking is slower at the edges of the spectrum to increase integration time. Thus, the resulting system efficiency is essentially compensated and is roughly constant. SNR is enhanced.

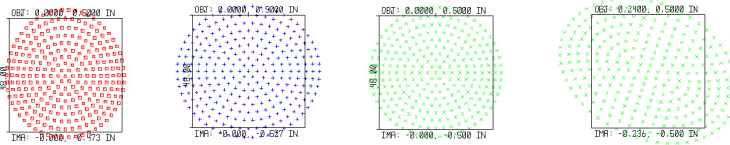
### Spot Size

The spot sizes calculated by Zemax in the hi-res mode are shown in Fig. 9. Note how they flatten out in the NIR actually giving higher spectral resolution. The box is 2 by 2 pixels.



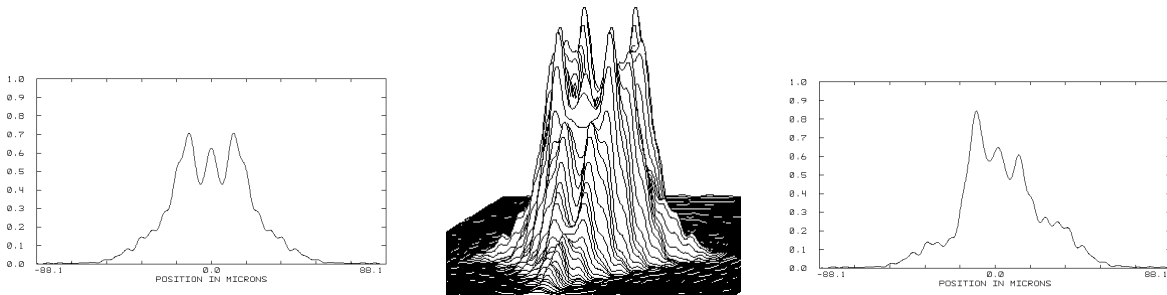
**Figure 9. Spot sizes from 290nm to 1015nm in hi-res mode.**

UG was optimized for low-res mode at 580nm. Fig. 10 shows these results in red, green, and blue. The field positions are all at the center of the CCD. The rightmost is 580nm but at the edge of the CCD showing increased off-axis distortion.. The focal positions of the optics were all adjusted to give the roundest spot in green.



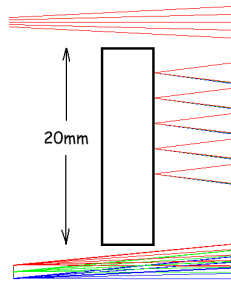
**Figure 10. Spot sizes from 290nm to 870nm in lo-res mode.**

One of the approximations in the above analysis was that the center ray of the incoming cone hit the center of the grating. This is not true, since to simplify mechanics, the input beam was taken parallel to the axis. After a dummy surface was inserted to put the stop in the correct position (for parallel input) the spot became a little more assymmetric. The x and y axis profiles are given in Fig. 11.



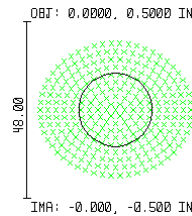
**Figure 11. Spot profiles for x and y axis.**

Fig. 12 shows how the new beam ends up hitting the grating off-center (about 0.093'' up). The effect is not very significant. If the grating were moved all the way back to the focal distance of 4'' the problem would go away.



**Figure 12. Off axis beam on grating.**

All of the above spots were taken a  $f/10$ . Nominal spot radius was  $20\mu\text{m}$  center and  $26\mu\text{m}$  edge. This is a little on the large side as the optimum spot has a FWHM equal to the pixel spacing ( $24\mu\text{m}$ ). Fortunately, at  $f/14$  the spot shrinks even more with less aberration to  $14\mu\text{m}$  in the center which is nearly optimal. In fact the optics start converging on the diffraction limit of an airy disk. The ratio is shown in Fig. 13.



**Figure 13. Spot size at  $f/14$  compared to airy disk.**

The effect of large spots is seen in the comparison plots of Fig. 14. On the left is the overlap of three input waves spaced  $10\text{nm}$  apart. Once mixed on the CCD it will appear as a total blur. On the right are spots at  $f/14$ , clearly better.

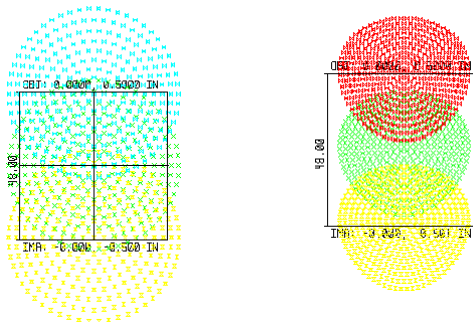


**Figure 14. Resolvability of spots of adjacent wavelengths.**

### Depth of Focus

There is spherical aberration which causes a de-focus of the spot. Outer rays do not converge at the same plane as the inner rays. Fig. 15 shows the beam (slightly angled out of page) through focus and the various spot shapes, each  $0.020''$  apart.

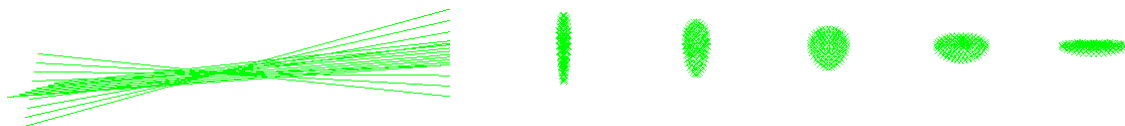


**Figure 15. Through focus and spot shape.**

Depth of field is quite large at f/10. Fig. 16 is a plot of spot size versus focus distance. Each grid is 0.005".

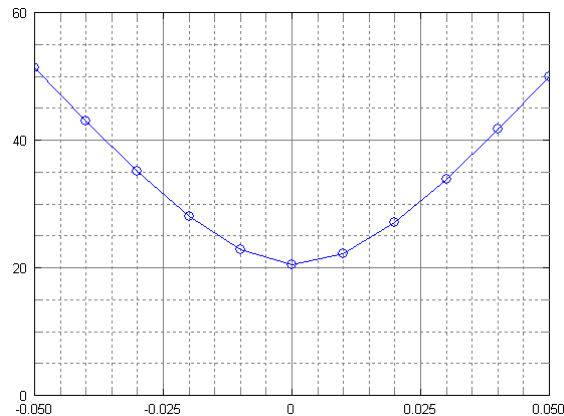


**Figure 16. Depth of field.**

### Thermal

The primary mirror is made of pyrex with a linear expansion coefficient of  $3.25 \times 10^{-6}/\text{C}$ . Our nominal operating range is  $20\text{C} \pm 20\text{C}$ . It is important that the instrument stays focused over this temperature range and that it gradually (not abruptly) loses focus at temperature extremes. For a  $\pm 20\text{C}$  change in temperature, the focus of the primary mirror will change by  $\pm 0.00026''$ , well below our depth of field.

Assuming an aluminum chassis, the linear coefficient of expansion would be  $33 \times 10^{-6}/\text{C}$ , about 10 times greater. This gives a thermal focal change of  $\pm 0.003''$ , still not a problem.

### Stray Light

One problem with a diffraction grating is that there is a lot of energy in the unused orders that ends up going every which way inside a spectrograph. That is why some instruments use dual slits. Zemax does not easily do a stray light analysis, but through brute force dozens of simulations were run to check the effects of stray light bouncing between the grating a primary several times. Fig. 17 shows where the 0<sup>th</sup> order goes, below the CCD onto the controller circuit board.

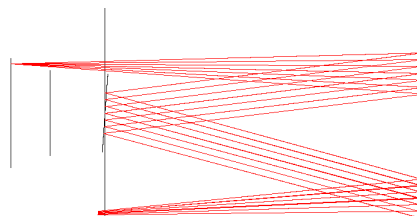


**Figure 17. Zero order position.**

Fig. 18 shows a few examples of some of the other simulations. Luckily, in each case the unwanted stray light was out of focus at the detector, most orders went back up towards slit. There will be some loss of contrast but the spread of energy reduces the problem.

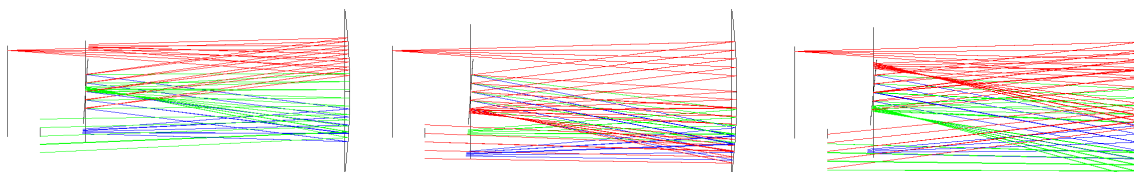


**Figure 18. Stray light is out of focus at detector.**